Hindawi
Mathematical Problems in Engineering
Volume 2017, Article ID 7189803, 11 pages
https://doi.org/10.1155/2017/7189803

Research Article

A Fisher's Criterion-Based Linear Discriminant Analysis for Predicting the Critical Values of Coal and Gas Outbursts Using the Initial Gas Flow in a Borehole

Xiaowei Li,[1,2] Chenglin Jiang,[1,2] Jun Tang,[1,2] Yujia Chen,[1,2] Dingding Yang,[1,2] and Zixian Chen[1,2]

[1]*Key Laboratory of Coal Methane and Fire Control, Ministry of Education, China University of Mining and Technology, Xuzhou, Jiangsu 221116, China*
[2]*School of Safety Engineering, China University of Mining and Technology, Xuzhou, Jiangsu 221116, China*

Correspondence should be addressed to Xiaowei Li; lixiaowei@cumt.edu.cn

Received 28 May 2016; Revised 18 August 2016; Accepted 10 October 2016; Published 11 May 2017

Academic Editor: Luis M. López-Ochoa

The risk of coal and gas outbursts can be predicted using a method that is linear and continuous and based on the initial gas flow in the borehole (IGFB); this method is significantly superior to the traditional point prediction method. Acquiring accurate critical values is the key to ensuring accurate predictions. Based on ideal rock cross-cut coal uncovering model, the IGFB measurement device was developed. The present study measured the data of the initial gas flow over 3 min in a 1 m long borehole with a diameter of 42 mm in the laboratory. A total of 48 sets of data were obtained. These data were fuzzy and chaotic. Fisher's discrimination method was able to transform these spatial data, which were multidimensional due to the factors influencing the IGFB, into a one-dimensional function and determine its critical value. Then, by processing the data into a normal distribution, the critical values of the outbursts were analyzed using linear discriminant analysis with Fisher's criterion. The weak and strong outbursts had critical values of 36.63 L and 80.85 L, respectively, and the accuracy of the back-discriminant analysis for the weak and strong outbursts was 94.74% and 92.86%, respectively. Eight outburst tests were simulated in the laboratory, the reverse verification accuracy was 100%, and the accuracy of the critical value was verified.

1. Introduction

Coal is the main nonrenewable energy resource consumed in China. Due to the advancement of coal mining in recent years, mining depths have reached 1,300 m and are estimated to reach 1,500 m within the next 20 years [1, 2]. As mining depth increases, ground stress as well as the pressure and content of gas in coal seams will increase, causing a corresponding increase in the outburst risk in coal seams. Outburst prediction is an important aspect of outburst coal seam mining to prevent accidents. For example, a serious accident occurred in 2011 in Sizhuang coal mine of Yunnan in China; the accident resulted in 43 deaths. Therefore, seam-mining countries around the world have all conducted extensive studies on outburst prediction. Outburst prediction methods can be divided into two categories: a single or comprehensive index and applying a statistical mathematical model.

In terms of the single or comprehensive index, the former Soviet Union proposed a Π_0-based comprehensive index method and a Π_e-based comprehensive index method [3] that were applied successively. Later, the Chinese researcher Wang [4] proposed a four-factor comprehensive index method involving the K value. Based on this method, the Fushun Institute of Coal Science [5, 6] of China proposed a comprehensive [6] index method involving the D and K values. Subsequently, the coal research and development institutes in China proposed a method involving the drill cutting desorption indexes Δh_2 and K_1. Jiang [7, 8] proposed a method based on the initial gas expansion energy released (IGEER). In addition, other countries have used index

methods involving V_1 [9] and $\Delta P_{\text{express}}$ [10]. All of the aforementioned methods measure the outburst risk at a certain point and use one point to represent the whole coal mass; in other words, they assume that the outburst risk in the predicted area is consistent with the outburst risk at the measured point. However, a coal mass is not a homogeneous body, making point prediction greatly limited.

Many factors can influence outburst prediction. Some researchers have used mathematical models to improve the accuracy of outburst prediction. Hao and Yuan [11], Tian and Zhou [12], and Qu et al. [13] studied the neural network model of outburst prediction. These methods are trained to capture the correlation between the outburst factors and the prominent outburst. To improve the accuracy of outburst prediction, Zhu et al. [14] combined principal component analysis (PCA) with the neural network. Zhang and Li [15] studied pattern recognition and the possibility prediction of coal and gas outbursts. With eight factors as the main discriminant, the pattern recognition method was used to perform possibility prediction of coal outbursts. Wang [16] studied the coal and gas outburst prediction based on fuzzy matter-element analysis. Guo et al. [17] studied the prediction method of coal and gas outbursts using the analytic hierarchy process and fuzzy comprehensive evaluation. The prediction of coal and gas outbursts was also studied using the analytic hierarchy process (AHP) and fuzzy comprehensive evaluation. In the prediction method, AHP was used to confirm the weights of the coal and gas outburst factors; the judgment matrix of each factor was constructed by membership functions; and the prediction model of coal and gas outbursts was established using the fuzzy comprehensive evaluation method. Zhao and Tan [18] studied the premonitory time series prediction of coal and gas outbursts based on chaos theory. According to the chaos characteristic of outburst prediction data, the outburst prediction model was established using the method of chaotic prediction. In addition, Peng and Wang [19] studied the improved analytic hierarchy process for coal and gas outburst prediction. Because the initial gas flow in the borehole (IGFB) is affected by many factors, and some of these factors are connected with each other while others are relatively independent, the IGFB are fuzzy and chaotic. These studies can be used as valuable references. However, the critical value of an outburst is usually measured under the simplest conditions. In the same way, research on the IGFB has discarded some minor factors. The fuzziness and chaos are relatively less. In addition, these methods are based on the results of point predictions and share the same disadvantages. Therefore, there are differences between research into the IGFB and the references.

The method established in the present study, which is based on the IGFB, is a linear prediction method. The mechanism of this method is as follows: during drilling, the volume of gas released from the borehole is continuously measured. Through data processing, the measured volume is converted to the total volume of gas released from a 1 m long borehole with a diameter of 42 mm within 3 min. The larger this flow is, the higher the outburst risk of the coal seam is. This method can continuously predict the outburst risk of coal seams passed during the drilling process. Therefore, this is a neoteric prediction method.

Wang and Yu [20–22] first analyzed such indexes in terms of the volume of drill cuttings and the volume of gas emitted from the borehole and found that the measured volume of gas emitted from the borehole exhibited fractal dimension characteristics. Based on Wang and Yu's study, Han [23], Qin et al. [24], Nie [25, 26], and Yuan [27] studied the borehole wall and the emission pattern of coal cuttings and gas during the drilling process. Based on the aforementioned studies, Wu [28] completed comprehensive laboratory and field application studies on the outburst risk prediction during the tunneling of soft coal seams and roadways using the continuous flow method; however, because of the complexity of field studies on outbursts, Wu obtained only the safety value of IGFB (32.30 L).

These studies show that IGFB is influenced by many factors, such as the degree of coal deformation, the gas permeability coefficient, the borehole diameter, the gas pressure, and the radius in front of the drill bit. Therefore, IGFB also has the characteristics of fuzziness and chaos. However, in studying the critical value of IGFB, we can change some influencing factors to build a research model under the most dangerous conditions. This model is an ideal rock cross-cut coal uncovering model. The effect of coal weight is neglected in this model. If the barrier layer is assumed to be dense and hard rock, then the amount of gas in the soft coal that leaks through the barrier into the tunnel is approximately zero. Then, the gas pressure in various locations in the soft coal remains at the initial pressure. Thus, regardless of the length of the driving cycle footage, the surface gas pressure in the exposed coal body after uncovering is equal to the initial gas pressure, and the outburst risk is at its highest level. Ideal rock cross-cut coal uncovering occurs under this condition, as shown in Figure 1. This condition also has the highest probability of outburst; using this outburst risk as the basis for prediction, the conditions are more stringent, thus achieving a higher safety margin. All of the tests in this study were conducted with this condition.

The model fully considers the mechanical properties of coal, the in situ stress of the coal seam, and the gas bearing. Therefore, the critical values obtained from this model are credible. Thus, the present study obtained sufficient sample data by establishing a stricter laboratory simulation system. The study also obtained critical values of weak and strong outbursts of IGFB using linear discriminant analysis based on Fisher's criterion. In addition, the present study also performed back-discriminant analysis and verification to determine the accuracy of the results.

2. Measurement of IGFB

The apparatus for measuring IGFB mainly consists of two parts: an oblong outburst coal seam simulation device and a flow measurement device. Figure 2 shows the mechanism used in the apparatus.

The experimental apparatus shown in Figure 2 contains three gas outflow channels: a flow sensor channel (channel 1),

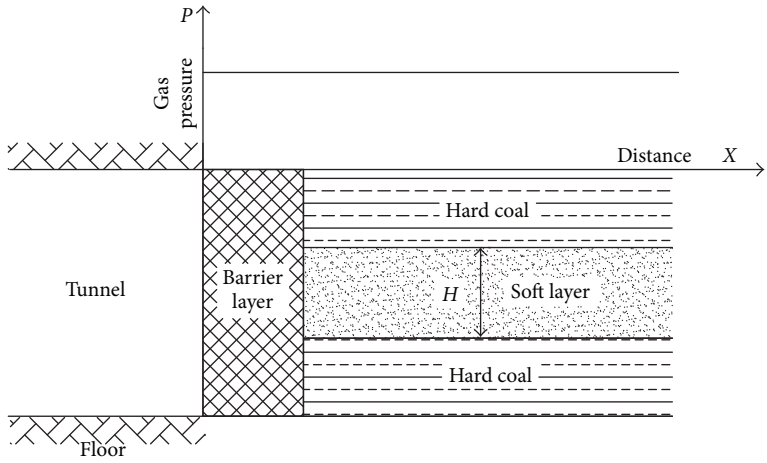

Figure 1: Gas pressure distribution in soft coal with a gas-to-barrier permeability coefficient of zero.

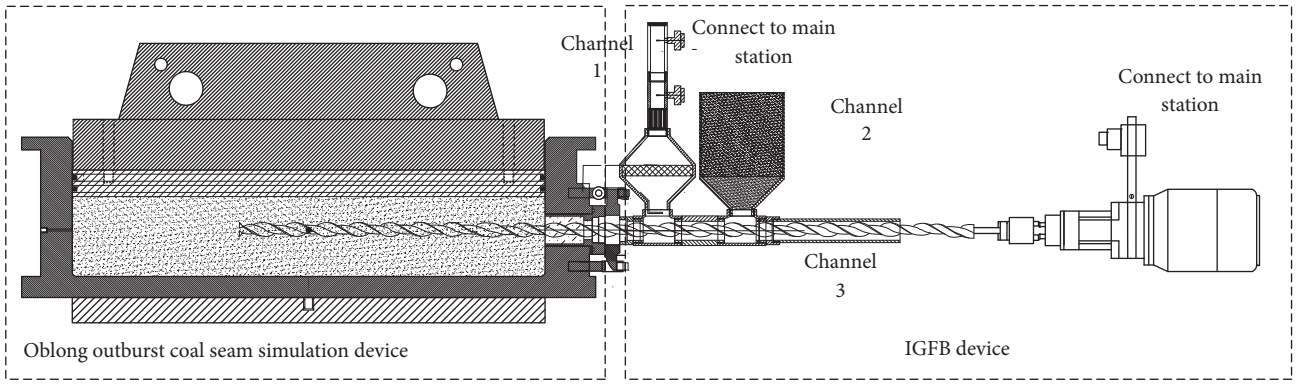

Figure 2: Laboratory IGFB measurement device.

a sealed coal chamber channel (channel 2), and a discharge channel for coal cuttings (channel 3). During the drilling process, the volume of gas emitted from the borehole that passes through channel 1 must be maximized and measured, while the volume of gas that passes through channel 2 and channel 3 must be minimized. Through experimentation, Wang et al. [29] demonstrated that the leakage of channel 2 and channel 3 is less than 1% and is negligible under the following conditions: the rotation speed is less than 425 r/min, channel 3 has a diameter of less than 60 mm and a length greater than 650 mm, and channel 2 is filled with coal cuttings with a diameter of less than 1 mm. The present study used a twist drill with a diameter of 42 mm for drilling and an electric coal drill with a rotation speed of 425 r/min to provide power; the length of channel 3 was set to 700 mm. Figure 3 shows the experimental configuration.

Coal samples from five coal mines in China were selected in the present study. A total of 48 sets of data were obtained, of which 23 sets were obtained under CO_2 conditions and 25 sets were obtained under N_2 conditions.

3. Analysis of the Range of IGFB Critical Values

After the data were collected, the IGEER from the coal samples was measured to determine the corresponding outburst risk. The IGEER is a comprehensive index for predicting coal seam outbursts [30, 31]. This index has been used to determine the outburst risk of 867 coal seams in 476 pairs of mine pits in China and has predicted the outburst risk of the coal seams with relative accuracy. Weak and strong outbursts have critical values of 42.98 mJ/g and 103.8 mJ/g, respectively. These critical values were used to determine the outburst risk of the simulated coal seams; Table 1 lists the results, and Figure 4 shows their distribution.

Figure 4 shows that a boundary exists between the nonoutburst samples and the weak outburst samples as well as between the weak outburst samples and the strong outburst samples. Based on the intervals between the boundaries, the critical values of the weak outbursts range from 35.28 to 38.26 L, and the critical values of the strong outbursts range from 77.56 to 86.94 L. To obtain accurate critical values, an

Table 1: The outburst danger of simulated coal seams under IGFB.

Sequence number	Coal sample	Gas type	Pressure (MPa)	IGFB (L)	IGEER (mJ/g)	Outburst type	Statistic $\sqrt[3]{Q}$
1	Xuehu coal mine, Henan, China	N_2	0.208	8.39	12.32	A	2.032
2		N_2	0.606	26.06	35.89	A	2.9648
3		CO_2	0.219	35.28	41.5	A	3.2798
4	Fenghui coal mine, Shanxi, China	N_2	0.21	15.34	18.7	A	2.4847
5	Wangchao coal mine, Shandong, China	N_2	0.594	13.47	16.48	A	2.3793
6		N_2	0.719	17.28	19.95	A	2.5853
7		CO_2	0.188	33.48	23.09	A	3.223
8		N_2	0.85	18.17	23.59	A	2.629
9		N_2	0.978	22.11	27.14	A	2.8067
10		N_2	1.186	32.26	32.91	A	3.1834
11	Wuzhong coal mine, Hebei, China	N_2	0.170	9.00	9.08	A	2.0801
12		N_2	0.331	13.32	17.69	A	2.3705
13		N_2	0.473	20.61	25.27	A	2.7417
14		CO_2	0.192	42.46	26.12	A	3.4887
15		N_2	0.778	31.14	41.57	A	3.1461
16	Yiluo coal mine, Henan, China	N_2	0.392	14.99	12.87	A	2.4657
17		CO_2	0.182	33.34	21.71	A	3.2185
18		N_2	0.759	20.44	24.92	A	2.7342
19		N_2	1.072	32.02	35.19	A	3.1755
20		N_2	1.225	33.59	40.22	A	3.2265
1	Xuehu coal mine, Henan, China	N_2	0.951	42.57	56.32	B	3.4917
2		CO_2	0.394	71.22	74.66	B	4.1451
3		N_2	1.436	98.18	85.04	B	4.6133
4	Fenghui coal mine, Shanxi, China	N_2	0.534	28.7	47.55	B	3.0617
5	Fenghui coal mine, Shanxi, China	CO_2	0.198	38.26	66.76	B	3.3696
6		N_2	0.797	52.31	70.96	B	3.7399
7		N_2	1.160	61.05	103.29	B	3.9376
8	Wangchao coal mine, Shandong, China	CO_2	0.409	51.4	50.24	B	3.7181
9		CO_2	0.596	70.98	73.21	B	4.1404
10		CO_2	0.766	77.56	94.09	B	4.2646
11	Wuzhong coal mine, Hebei, China	CO_2	0.320	53.3	43.54	B	3.7634
12		N_2	1.076	56.97	57.49	B	3.8478
13		N_2	1.473	72.37	78.7	B	4.1673
14		CO_2	0.605	103.33	82.31	B	4.6925
15	Yiluo coal mine, Henan, China	CO_2	0.369	39.17	44.01	B	3.3961
16		N_2	1.468	50.63	48.19	B	3.6994
17		CO_2	0.591	52.98	70.49	B	3.7558
18		CO_2	0.766	72.9	91.36	B	4.1774
1	Xuehu coal mine, Henan, China	CO_2	0.612	92.59	115.97	C	4.524
2		CO_2	0.846	119.44	160.32	C	4.9247
3		CO_2	1.019	143.02	193.1	C	5.2296
4	Fenghui coal mine, Shanxi, China	CO_2	0.407	115.45	137.22	C	4.8693
5		N_2	1.674	117.24	149.05	C	4.8943
6		CO_2	0.622	170.38	209.71	C	5.5438
7		CO_2	0.796	270.69	268.38	C	6.4688

Table 1: Continued.

Sequence number	Coal sample	Gas type	Pressure (MPa)	IGFB (L)	IGEER (mJ/g)	Outburst type	Statistic $\sqrt[3]{Q}$
8	Wangchao coal mine, Shandong, China	CO_2	1.033	115.22	126.88	C	4.866
9	Wuzhong coal mine, Hebei, China	CO_2	0.765	152.6	104.08	C	5.3438
10	Yiluo coal mine, Henan, China	CO_2	0.919	86.94	109.61	C	4.43

A: nonoutburst; B: weak outburst; C: strong outburst; resorted according to types A, B, and C.

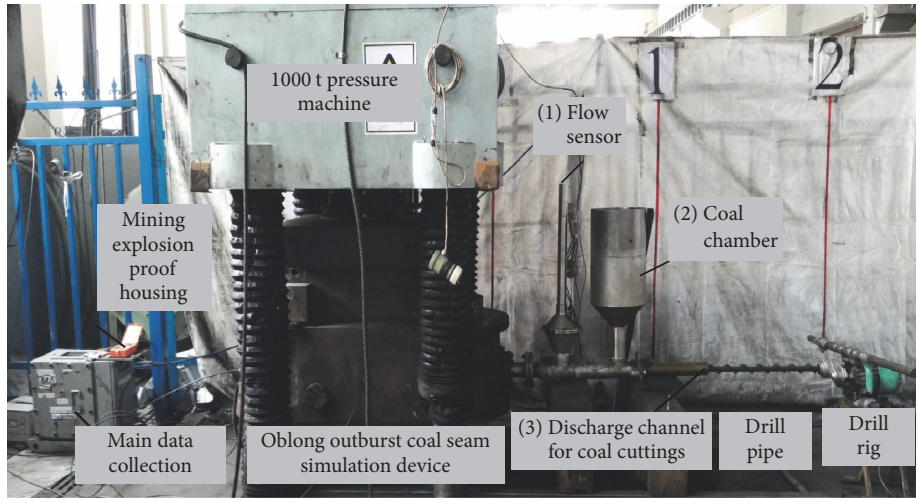

Figure 3: IGFB measurement device.

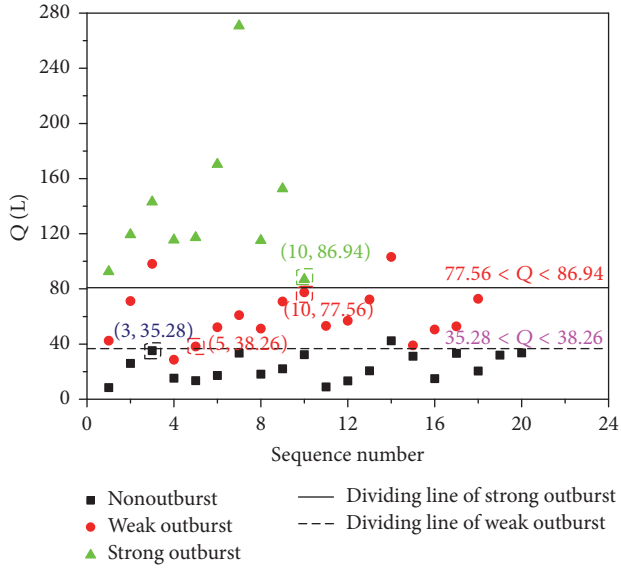

Figure 4: IGFB measurement results of coal seams with different levels of outburst risk.

accurate discriminant analysis must be performed. Figure 3 shows that the boundaries are linear; therefore, the critical values can be determined using linear discriminant analysis based on Fisher's criterion.

4. Linear Discrimination Based on Fisher's Criterion

Fisher's discrimination method is commonly used in multivariate statistical discriminant analysis. The basic idea of Fisher's discrimination method is projection. Assume that A and B are two ensembles, n_1 samples are taken from A, and n_2 samples are taken from B. Then, p discriminant indexes are measured for the samples taken from A and the samples taken from B. A linear discriminant function, $y(x)$, that can reduce the data to a one-dimensional numerical value is determined:

$$y(x) = c_1 x_1 + c_2 x_2 + \cdots + c_p x_p, \quad (1)$$

where $c_1, c_2, \ldots, c_p$ are the coefficients to be determined and $x_1, x_2, \ldots, x_p$ are the measured values of the indexes.

Then, the linear function is used to transform the samples of the known class and the class of knowledge into one-dimensional data in dimension P. According to the degree of affinity, it is possible to identify the attribution of unknown samples. This linear function transforms all the points in P-dimensional space into one-dimensional numerical values. It can not only reduce the difference between samples of

the same class but also maximize the difference between sample points in different categories, which results in a higher discriminant efficiency. The calculation procedure is as follows.

First, the mean value and the covariance of the samples from group A and group B are calculated:

$$\overline{x_k}(A) = \frac{1}{n_1}\sum_{i=1}^{n_1} x_{ki}(A),$$

$$\overline{x_k}(B) = \frac{1}{n_2}\sum_{i=1}^{n_1} x_{ki}(B) \quad (k = 1, 2, \ldots, p), \tag{2}$$

$$S_{kl} = \sum_{i=1}^{n_1}\left(x_{ki}(A) - \overline{x_k}(A)\right)\left(x_{kl}(A) - \overline{x_l}(A)\right) + \sum_{i=1}^{n_2}\left(x_{ki}(B) - \overline{x_k}(B)\right)\left(x_{kl}(B) - \overline{x_l}(B)\right).$$

Let $d_k = \overline{x_k}(A) - \overline{x_k}(B)$, $(k = 1, 2, \ldots, p)$ and $D = (d_1, d_2, \ldots, d_p)'$. Based on $SC = D$, the coefficient matrix, C, is calculated to obtain the discriminant function. Then, $\overline{y}(A)$ and $\overline{y}(B)$ are calculated using n_1 type A samples and n_2 type B samples, respectively:

$$\overline{y}(A) = \sum_{r=1}^{p} c_r \overline{x_r}(A),$$

$$\overline{y}(B) = \sum_{r=1}^{p} c_r \overline{x_r}(B). \tag{3}$$

Finally, the weighted average of $\overline{y}(A)$ and $\overline{y}(B)$ is used as the critical value of the discriminant function:

$$y_c = \frac{n_1\overline{y}(A) + n_2\overline{y}(B)}{n_1 + n_2}. \tag{4}$$

Each sample that fulfills $y = c_1x_1 + c_2x_2 + \cdots + c_px_p < y_c$ belongs to type A; otherwise, the sample belongs to type B.

This discriminant analysis assumes that the two groups of samples are taken from different ensembles. If the difference in the mean value is insignificant, then the discrimination is of no value. Therefore, it is necessary to test whether there is a significant difference between the two ensembles. The test statistic is constructed based on the Mahalanobis distance (D^2):

$$F = \left[\frac{n_1n_2}{(n_1 + n_2)(n_1 + n_2 - 2)}\right]\left(\frac{n_1 + n_2 - p - 1}{p}\right) \cdot (n_1 + n_2 - 2)\sum_{i=1}^{p} c_id_i, \tag{5}$$

where

$$D^2 = (n_1 + n_2 - 2)\sum_{i=1}^{p} c_id_i. \tag{6}$$

The statistic F follows the F distribution with p and $n_1 + n_2 - p - 1$ degrees of freedom, that is, $F(p, n_1 + n_2 - p - 1)$. The test value of statistic F is obtained from (5). Using the F distribution table, $F_\alpha(p, n_1 + n_2 - p - 1)$ is obtained, where α represents the test significance level ($\alpha = 0.05$ or 0.01). The value of F is compared with the value of $F_\alpha(p, n_1 + n_2 - p - 1)$ to determine whether there is a significant difference between the two ensembles.

5. Linear Discriminant Analysis of the Critical Values of Outbursts Predicted Using IGFB

5.1. Normal Transformation of the Statistic. When statistic F is used for the discriminant analysis of two types of samples, the samples must follow a normal distribution. The histogram method is the most visual method for determining whether samples follow a normal distribution. The number of small statistic intervals in a histogram is generally determined using the following equation [32]:

$$m_0 = 1.87(n - 1)^{2/5}, \tag{7}$$

where m_0 is the number of small statistic intervals and n is the number of data points or samples.

Normalization was required for both of the sample combinations measured in the present study. A cubic root transformation was applied to the original data. Based on Table 1 and (7), there were 38 nonoutburst and weak outburst samples (the number of small intervals was set to 8) and 28 weak and strong outburst samples (the number of small intervals was set to 7). Based on these results, histograms were plotted, as shown in Figure 5. After transformation, the data approximately followed a normal distribution and thus could be used for discriminant analysis.

5.2. Discriminant Calculation and the Test of the Critical Values of the Outbursts. The number of nonoutburst samples and the number of weak outburst samples were $n_1 = 20$ and $n_2 = 18$, respectively, and their mean values were $\overline{x}(A) = 2.8108$ and $\overline{x}(B) = 3.8879$, respectively. The sum of the covariances of the two sets of samples was $s = 6.7972$, and $d = \overline{x}(B) - \overline{x}(A) = 1.0771$. The coefficient of the discriminant function was $c = d/s = 0.1585$, and the critical value determined based on the discriminant function was

$$y_c = \frac{n_1c\overline{x}(A) + n_2c\overline{x}(B)}{n_1 + n_2} = 0.5264. \tag{8}$$

Because the IGFB was the only prediction index, $p = 1$. The discriminant function is $y = cx$, where $x = \sqrt[3]{Q}$. Therefore, the critical value of the weak outbursts obtained was as follows: $Q_C = (y_c/c)^3 = 36.63$ L. Thus, there was no outburst risk when the flow was less than 36.63 L; otherwise, there was a weak outburst risk or a strong outburst risk. When $p = 1$, we obtained

$$D^2 = (n_1 + n_2 - 2)cd = (n_1 + n_2 - 2)c[\overline{x}(B) - \overline{x}(A)]. \tag{9}$$

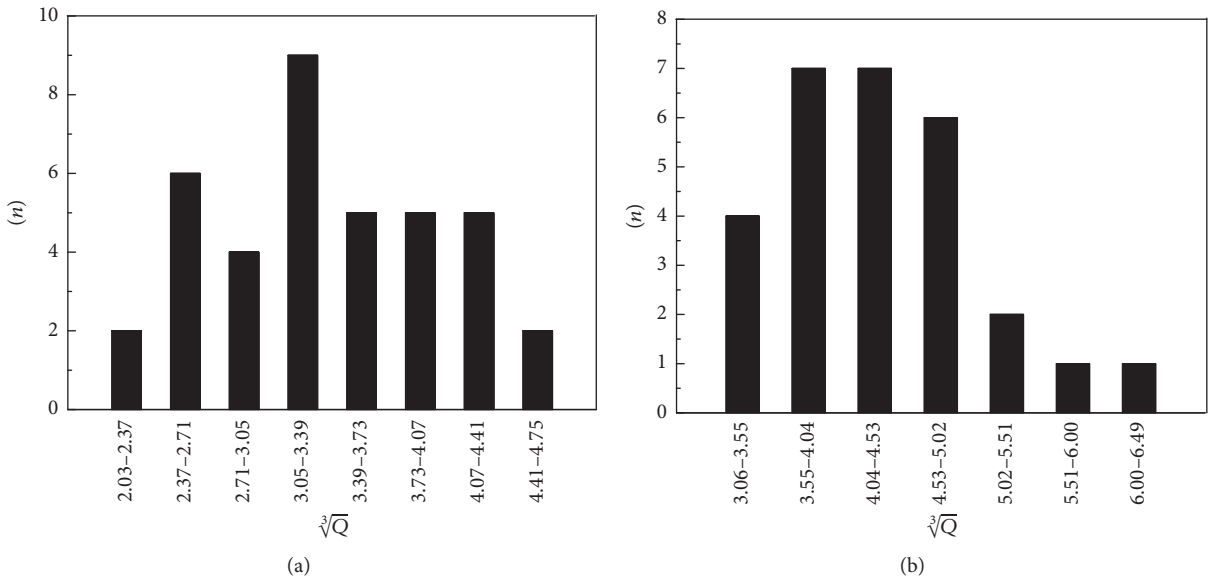

FIGURE 5: Sample histogram of $\sqrt[3]{Q}$ ((a) samples of nonoutbursts and weak outbursts and (b) samples of weak outbursts and strong outbursts).

The statistic used for examination was

$$F = \frac{n_1 n_2}{n_1 + n_2} (n_1 + n_2 - 2)\, c\, [\overline{x}(B) - \overline{x}(A)]. \quad (10)$$

Through calculation, the test value of the statistic was determined to be $F = 58.22$. Using the F distribution table, we obtained

$$F_\alpha (p, n_1 + n_2 - p - 1) = F_{0.01}(1, 36) = 7.39. \quad (11)$$

Because coal and gas outbursts are very dangerous, the prediction error will cause serious consequences. Therefore, a higher degree of confidence value should be selected; $\alpha = 0.01$ was used for a confidence level of the sample of 99%. Because $F_1 = 58.22 > F_{0.01}(1, 36) = 7.39$, there was a significant difference between the mean values of the two sets of variables, and the discrimination was valid.

Similarly, the number of weak outburst samples and the number of strong outburst samples were $n_2 = 18$ and $n_3 = 10$, respectively, and the mean value was $\overline{x}(C) = 5.1094$. The sum of the covariances of the two sets of samples was $s = 6.1866$. Additionally, $d = \overline{x}(C) - \overline{x}(B) = 1.2215$. The coefficient of the discriminant function was $c = d/s = 0.1974$. Therefore, the critical value of the strong outbursts was 80.85 L.

Through calculations, the test value of the statistic was determined to be $F = 40.30$. Using the F distribution table, we obtained

$$F_\alpha (p, n_1 + n_2 - p - 1) = F_{0.01}(1, 26) = 7.72. \quad (12)$$

Because $F = 40.30 > F_{0.01}(1, 26) = 7.72$, there was a significant difference between the mean values of the two sets of variables, and the discrimination was valid.

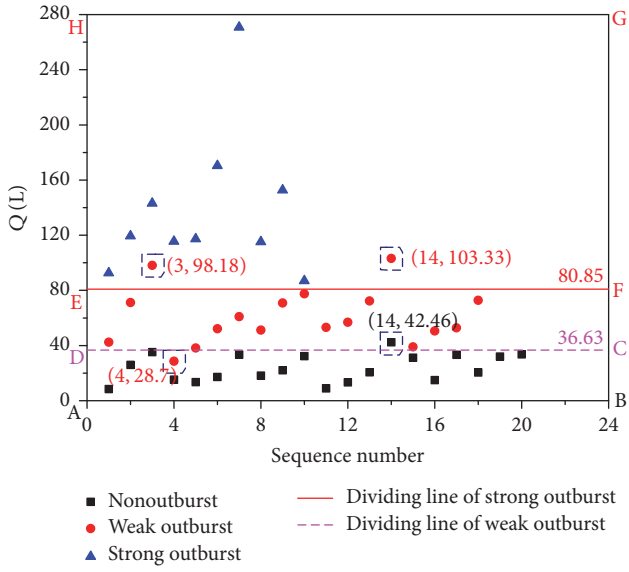

FIGURE 6: Back-discrimination of the discriminant analysis.

5.3. Back-Discriminant Analysis of the Critical Values. The back-discriminant analysis of the discriminant analysis results was performed according to the following process: the critical values (i.e., 36.63 L and 80.85 L) were used to determine the outburst risk. In addition, the index method involving the IGEER index was also used to determine the outburst risk. If the two determination results were consistent, the sample point was classified as a normal point; otherwise, the sample point was classified as an anomalous point, and the back-discrimination was erroneous. Figure 6 shows the back-discrimination results.

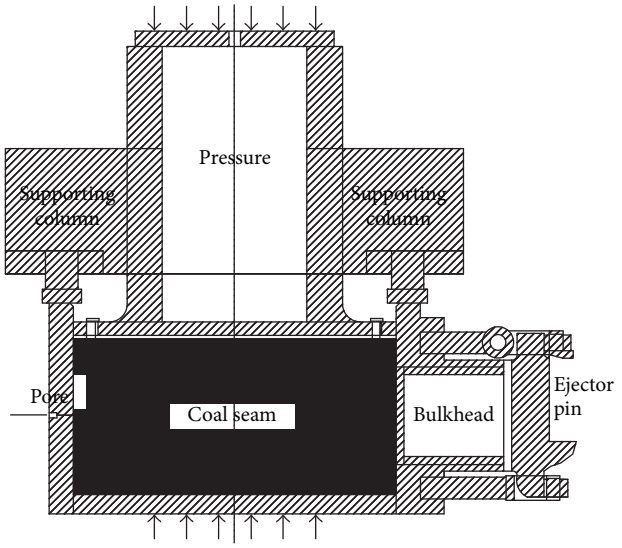

Figure 7: Outburst simulation test system.

In Figure 6, the critical values divided the 48 samples into three sections. The sample points within the dotted line boxes were anomalous points. There was one anomalous point in the nonoutburst section ABCD (4, 28.70 L); one anomalous point in the weak outburst section CDEF (14, 42.46 L); and two anomalous points in the strong outburst section EFGH (3, 98.18 L) and (14, 103.33 L). Therefore, the outburst and weak outburst samples were back-discriminated 38 times, and the back-discrimination was erroneous twice (correct back-discrimination rate: 94.74%). The weak and strong outburst samples were back-discriminated 28 times, and the back-discrimination was erroneous two times (correct back-discrimination rate: 92.86%). The correct back-discrimination rates were all above 90%. The high rates of correct back-discrimination indicate that the critical values obtained from the discriminant analysis were accurate.

6. Verification of the IGFB Critical Values in the Laboratory

Because of the rarity of outbursts, field verification of the above critical values is challenging. Therefore, to verify the accuracy of the above results, outburst simulation tests were conducted in the laboratory. Figure 7 shows the experimental device.

Each coal seam was compressed five times during the simulation process. After compression, each coal seam was subjected to vacuum pumping for 12 h and then filled with gas. Prior to filling each coal seam with gas, the initial gas flow and the gas pressure in the borehole were fitted, and the fitting function was obtained. Figure 8 shows the resulting fitting curves. By substituting the critical values (i.e., 36.63 L and 80.85 L) into the fitting curves, the gas filling pressure (P) was obtained. The gas filling process was performed for more than 48 h to attain adsorption equilibrium. However, because the adsorption process was relatively complex, it could not

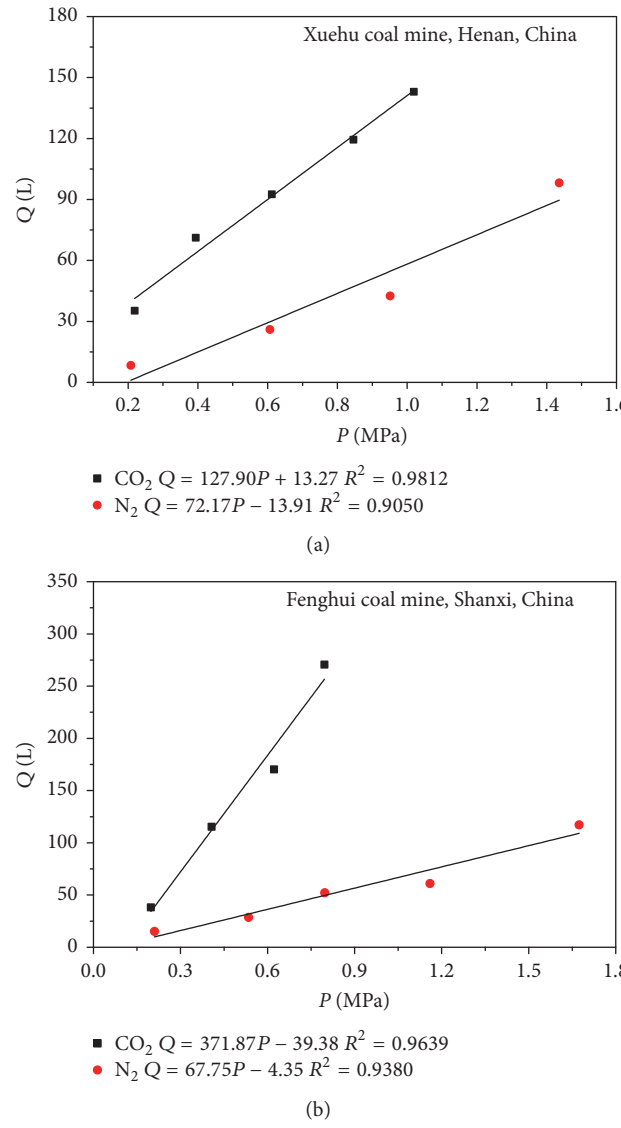

Figure 8: Relationship between the IGFB and gas pressure of Xuehu and Fenghui coal mines.

be guaranteed that the gas filling pressure was equal to the critical value. Therefore, the flow was indirectly calculated based on the equilibrium pressure during the determination process.

The gas dynamic phenomena were classified into three types in the outburst simulation: nonoutbursts, weak outbursts, and strong outbursts. For the nonoutbursts, the percentage of the volume of the collapsed coal in the total volume of the coal (referred to as the "throw-out ratio") was 0–5%. For the weak outbursts, the coal wall was damaged, and the throw-out rate was 5–40%. For the strong outbursts, there was an intense gas dynamic phenomenon, and the throw-out rate was more than 40%. Eight simulation tests were conducted (Table 2); Figure 9 shows a photograph of some of the tests.

In each of the eight simulation tests, the actual dynamic phenomenon of the coal seam was consistent with the

Table 2: The results of the outburst simulation experiments and IGFB prediction.

Sequence number	Coal sample	Gas type	Gas pressure (MPa)	Outburst situation	Throw-out rate (%)	Results of outburst simulation	IGFB (L)	Predicted results of IGFB
1	Wangchao coal mine, Shandong, China	N_2	0.279	Coal wall without damage	0	Nonoutburst	2.95	Nonoutburst
2	Wuzhong coal mine, Hebei, China	N_2	0.326	Coal wall without damage	0	Nonoutburst	13.91	Nonoutburst
3	Fenghui coal mine, Shanxi, China	N_2	0.326	Coal wall with slight damage	0	Nonoutburst	17.74	Nonoutburst
4	Wuzhong coal mine, Hebei, China	CO_2	0.154	Coal wall without damage	0	Nonoutburst	27.74	Nonoutburst
5	Yiluo coal mine, Henan, China	CO_2	0.216	The quality of thrown coal is 2.1 kg	2.25	Nonoutburst	30.98	Nonoutburst
6	Xuehu coal mine, Henan, China	CO_2	0.216	The quality of thrown coal is 4.1 kg	5.13	Weak outburst	40.90	Weak outburst
7	Yiluo coal mine, Henan, China	CO_2	0.387	The quality of thrown coal is 8.1 kg	8.66	Weak outburst	43.75	Weak outburst
8	Fenghui coal mine, Shanxi, China	CO_2	0.346	The quality of thrown coal is 39.1 kg	40.54	Strong outburst	89.29	Strong outburst

(a) (b)

Figure 9: A photograph of the outburst simulation experiments ((a) Xuehu: weak outburst, 0.216 MPa, CO_2; (b) Fenghui: strong outburst, 0.346 MPa, CO_2).

outburst type determined based on the critical value of IGFB. This consistency indicates that the determined critical value was reliable.

7. Conclusions

(1) The initial gas flow released within 3 min from a 1 m long borehole with a diameter of 42 mm was measured in the laboratory; a total of 48 sets of data were obtained. The outburst risk corresponding to the IGFB was classified based on the critical values of the IGEER; 20 sets of nonoutburst data, 18 sets of weak outburst data, and 10 sets of strong outburst data were obtained.

(2) A linear discriminant analysis based on Fisher's criterion was established for IGFB. Through data normalization and analysis, the critical values of the weak and strong outburst risks were predicted using the method based on IGFB (36.63 L and 80.85 L, resp.). Furthermore, back-discriminant analysis was performed, and the accuracy was 94.74% and 92.86%, respectively.

(3) Eight simulation tests were conducted in the laboratory. The test results verified the accuracy of the critical values of the outbursts obtained using the method based on IGFB.

Conflicts of Interest

The authors declare that there are no conflicts of interest regarding the publication of this paper.

Acknowledgments

This paper was supported by the Natural Science Foundation of Jiangsu Province, China (Grants nos. BK20150195, BK20150180, and BK20150181), the Graduate Research and Innovation Projects of Jiangsu Province, China (Grant no. KYLX15-1431), and financial support from the Project Funded by the Priority Academic Program Development of Jiangsu Higher Education Institutions (PAPD).

References

[1] M.-C. He, H.-P. Xie, S.-P. Peng, and Y.-D. Jiang, "Study on rock mechanics in deep mining engineering," *Chinese Journal of Rock Mechanics and Engineering*, vol. 24, no. 16, pp. 2803–2813, 2005.

[2] H.-P. Xie, F. Gao, Y. Ju et al., "Quantitative definition and investigation of deep mining," *Journal of the China Coal Society*, vol. 40, no. 1, pp. 1–10, 2015.

[3] J. M. Li, *Technical Manuals of Coal and Gas Outburst Prevention and Control*, China University of Mining and Technology Press, Xuzhou, China, 2006.

[4] Y. A. Wang, *Technical Manuals of Coal Mine Safety*, China Coal Industry Press, Beijing, China, 1994.

[5] State Administration of Work Safety of China and State Administration of Coal Mine Safety of China, *Prevention and Control Regulations on Coal and Gas Outburst*, China Coal Industry Press, Beijing, China, 2009.

[6] State Administration of Coal Mine Safety of China, *Reader of Prevention and Control Regulations on Coal and Gas Outburst*, China Coal Industry Press, Beijing, China, 2009.

[7] C. L. Jiang and Q. X. Yu, "Spherical shell instability hypothesis of coal and gas outburst mechanism," *Safety in Coal Mines*, vol. 26, no. 2, pp. 17–25, 1995.

[8] C. L. Jiang, "Analyses on the developing process and mechanical conditions of coal and gas outburst front," *Journal of China University of Mining Technology*, vol. 23, no. 4, pp. 1–9, 1994.

[9] J. Toraño, S. Torno, E. Alvarez, and P. Riesgo, "Application of outburst risk indices in the underground coal mines by sublevel caving," *International Journal of Rock Mechanics and Mining Sciences*, vol. 50, pp. 94–101, 2012.

[10] O. Esen, S. C. Ozer, and A. Fisne, "Classification of coal seams for coal and gas outburst proneness in the Zonguldak Coal Basin," in *Proceedings of the 14th Coal Operators' Conference of Australasian Institute of Mining and Metallurgy & Mine Managers Association of Australia (COAL '14)*, University of Wollongong, Wollongong, Australia, 2014.

[11] J. S. Hao and C. F. Yuan, "The applying of fuzzy network techniques in prediction of coal and gas outbursts," *Journal of China Coal Society*, vol. 24, no. 6, pp. 624–627, 1999.

[12] Y. L. Tian and L. H. Zhou, "The study on the methods for predicting coal or gas outburst based on bp neural network," *System Engineering Theory and Practice*, vol. 24, no. 12, pp. 102–105, 2005.

[13] F. Qu, L. Zhang, and Y. Y. Li, "Development of coal and gas outburst prediction system based on bp neural network," *China Safety Science Journal*, vol. 22, no. 1, pp. 11–15, 2012.

[14] Z. J. Zhu, H. W. Zhang, and J. Han, "Prediction of coal and gas outburst based on PCA-BP neural network," *China Safety Science Journal*, vol. 23, no. 4, pp. 45–49, 2013.

[15] H. W. Zhang and S. Li, "Pattern recognition and possibility prediction of coal and gas outburst," *Chinese Journal of Rock Mechanics and Engineering*, vol. 24, no. 19, pp. 3577–3580, 2005.

[16] Y. J. Wang, *Based on Fuzzy Matter-Element Analysis of Coal and Gas Outburst Prediction*, Taiyuan University of Technology, Taiyuan, China, 2011.

[17] D. Guo, J. Fan, S. Ma, and Y. Wang, "Prediction method of coal and gas outburst by analytic hierarchy process and fuzzy comprehensive evaluation," *Journal of University of Science and Technology Beijing*, vol. 29, no. 7, pp. 660–664, 2007.

[18] Z.-G. Zhao and Y.-L. Tan, "Study of premonitory time series prediction of coal and gas outbursts based on chaos theory," *Rock and Soil Mechanics*, vol. 30, no. 7, pp. 2186–2190, 2009.

[19] H. Peng and X. Wang, "Improved analytic hierarchy process for coal and gas outburst prediction," *Journal of Liaoning Technical University: Natural Science*, vol. 34, no. 7, pp. 774–778, 2015.

[20] K. Wang, Q. X. Yu, and B. S. Zhou, "Prediction mechanism and analysis of prediction index of coal and gas outburst by drilling method," *Jiangsu Coal*, no. 2, pp. 13–15, 1995.

[21] K. Wang, Q. X. Yu, and L. W. Guo, "Dynamic characteristics of gas emission during boring and its relation with gas outburst danger," *Journal of China University of Mining Technology*, vol. 27, no. 3, pp. 257–260, 1998.

[22] K. Wang, Q.-X. Yu, and C.-L. Jiang, "Study of dynamic gas emission during boring process by using numerical simulation," *Journal of China Coal Society*, vol. 26, no. 3, pp. 279–284, 1998.

[23] Y. Han, *Research on Gas Emission Law of Borehole Wall and Drill Cuttings in Course of Drilling*, China University of Mining and Technology, Xuzhou, China, 2007.

[24] Y. P. Qin, P. Liu, and Y. J. Hao, "Finite difference model of borehole gas emission and numerical simulation," *Journal of Liaoning Technical University (Natural Science)*, vol. 33, no. 10, pp. 1297–1301, 2014.

[25] B. S. Nie, Y. Y. Guo, S. Y. Wu, and L. Zhang, "Theoretical model of gas diffusion through coal particles and its analytical soluion," *Journal of China University of Mining & Technology*, vol. 30, no. 1, pp. 21–24, 2001.

[26] Y. Han, F.-Y. Zhang, W.-F. Yu, and C.-L. Jiang, "Experimental study on gas diffusion law from drill cuttings during the whole desorption process," *Journal of the China Coal Society*, vol. 36, no. 10, pp. 1699–1703, 2011.

[27] J. W. Yuan, *Study on Time-Related Characteristics of Gas Diffusion from Particles Coal*, China University of Mining & Technology, Beijing, China, 2014.

[28] A. J. Wu, *Study on Technology of Continuous Flow about Outburst Hazard Prediction during Driving in Soft Coal Roadway*, China University of Mining and Technology, Xuzhou, China, 2011.

[29] G. D. Wang, C. L. Jiang, and A. J. Wu, "Dynamic separation technology of drill cutting and gas in continuous flow method," *Journal of Liaoning Technical University (Natural Science)*, vol. 31, no. 2, pp. 176–180, 2012.

[30] C. L. Jiang, "Prediction study of three dynamic force phenomena under the condition of uncovering coal seam in cross-cut," *Journal of China Coal Society*, vol. 22, no. 4, pp. 72–75, 1997.

[31] C. L. Jiang, "Linear discriminatory analysis on coal and gas outburst danger and its critical value," *Journal of China University of Mining & Technology*, vol. 29, no. 01, pp. 63–66, 2000.

[32] Q. Y. Wu and L. Ling, *Applied Mathematical Statistics*, Tianjin University Press, Tianjin, China, 2004.